Pergamon

PII: S0191-8141(97)00012-6

Journal of Structural Geology, Vol. 19, No. 5, pp. 653 to 661, 1997

0191-8141/97 $17.00+0.00

Development of a chevron cleavage pattern and porphyroblast rotation in graded metaturbidites, Slave structural province, Northwest Territories, Canada

J. R. HENDERSON

Geological Survey of Canada, Ottawa K1A 0E8, Canada

(*Received* 23 *August* 1996; *accepted in revised form* 18 *January* 1997)

Abstract—Chevron cleavage pattern displays opposite cleavage vergence across a psammite–pelite contact or within a single graded couplet. In this example, graded metaturbidites preserve an S_2 cleavage with dextral vergence in their competent psammitic bases, and an S_3 crenulation cleavage with sinistral vergence in their less-competent semi-pelitic tops. Bedding-parallel shear, partitioned into tops of graded couplets, resulted in buckle-folding of S_2 cleavage. S_3 is also a compositionally differentiated cleavage displaying alternating quartz-rich microlithons (Q) and muscovite-rich cleavage domains (M). Together, Q and M domains define S-microfolds related to D_3.

Biotite porphyroblasts, developed during static metamorphism before D_2/S_2, contain quartz-inclusion trails (S_{1i}) with three orientation patterns that are related to their location within graded beds. Porphyroblasts in psammitic bases of graded couplets are not affected by D_3/S_3. In comparison, S_{1i} in porphyroblasts in semi-pelitic tops of beds are, on average, about 5° clockwise in M domains, and about 90° counter-clockwise in Q domains, corresponding to flat and steep limbs of S-shaped microfolds in S_2. From these observations, it is apparent that biotite porphyroblasts within Q domains rotated about 90° counter-clockwise during microfolding. Within M domains, the S_{1i} data suggest that porphyroblasts rotated little, relative to their orientation in the base of the beds. © 1997 Elsevier Science Ltd.

INTRODUCTION

Chevron cleavage patterns can occur in metaturbidite beds that exhibit several generations of cleavage. They are common in metaturbidites of the Slave structural province, Northwest Territories, Canada (Fig. 1). Fyson (1982) introduced the term in reference to interbedded psammites and pelites in which the locally dominant foliation alternates with lithology from S_2 to S_3, producing a chevron pattern. With this pattern, the cleavages of different generation in contrasting lithologies form a mirror image about bedding with similar angles but opposite vergence relative to the bedding surface.

King and Helmstaedt (1989) describe a chevron cleavage pattern at Point Lake, Northwest Territories defined by NW-striking S_3 continuous cleavage in the psammitic bases of graded metaturbidites, and NE-striking S_4 crenulation cleavage in the pelitic tops of the graded beds. Kusky and De Paor (1991) re-examined the outcrop of chevron cleavage pattern described by King and Helmstaedt (1989), and questioned whether the chevron pattern might be explained by deformed cross-laminations in the pelitic tops of graded beds due to bedding-parallel simple shear.

Chevron cleavage pattern probably occurs in poly-deformed psammite–pelite couplets, as well as interbedded psammites and pelites elsewhere, but to my knowledge it has not been documented or analyzed. It is the intention here to describe another example of chevron cleavage pattern from Slave province metaturbidites, and to document an example of porphyroblast rotation related to crenulation cleavage development. In recent years there has been much debate concerning porphyroblast rotation (Vissers and Mancktelow, 1992) and non-rotation (Fyson, 1980; Bell, 1985; Bell and Johnson, 1992; Aerden, 1995) during folding. In this example, porphyroblast rotation occurred in quartz-rich, but not in mica-rich domains during contractional crenulation cleavage development by microfolding of an older continuous cleavage.

The beds studied (Fig. 2, north to the left) are exposed on horizontal surfaces normal to the line of intersection of the cleavages and bedding (S_0). The beds strike 360° and dip 90°. Their psammitic bases show a NW-striking, vertical S_2 continuous cleavage with dextral vergence relative to S_0, whereas silty pelite forming the tops of the graded beds has a NE-striking, vertical S_3 crenulation cleavage with sinistral vergence relative to S_0. The combination of S_2 and S_3 gives the weathered outcrop surface a chevron-like appearance. A prominent mm-scale ribbing is displayed by the weathered S_3 differentiated crenulation cleavage (Fig. 2), and is restricted to a few silty tops of turbidites at the specimen locality. Toward the bases of the graded couplets, the S_3 crenulation cleavage forms a progressively larger refraction angle with bedding, and disappears as the quartz content of the graded couplet increases.

REGIONAL GEOLOGICAL SETTING

The outcrop shown in Fig. 2 is located at the abandoned Ruth Gold Mine, about 90 km east of Yellowknife (Fig. 1) within Burwash Formation sandy turbidites of the Yellowknife Supergroup (Henderson, 1985). The Burwash Formation conformably overlies mafic to felsic metavolcanic rocks that lie unconformably

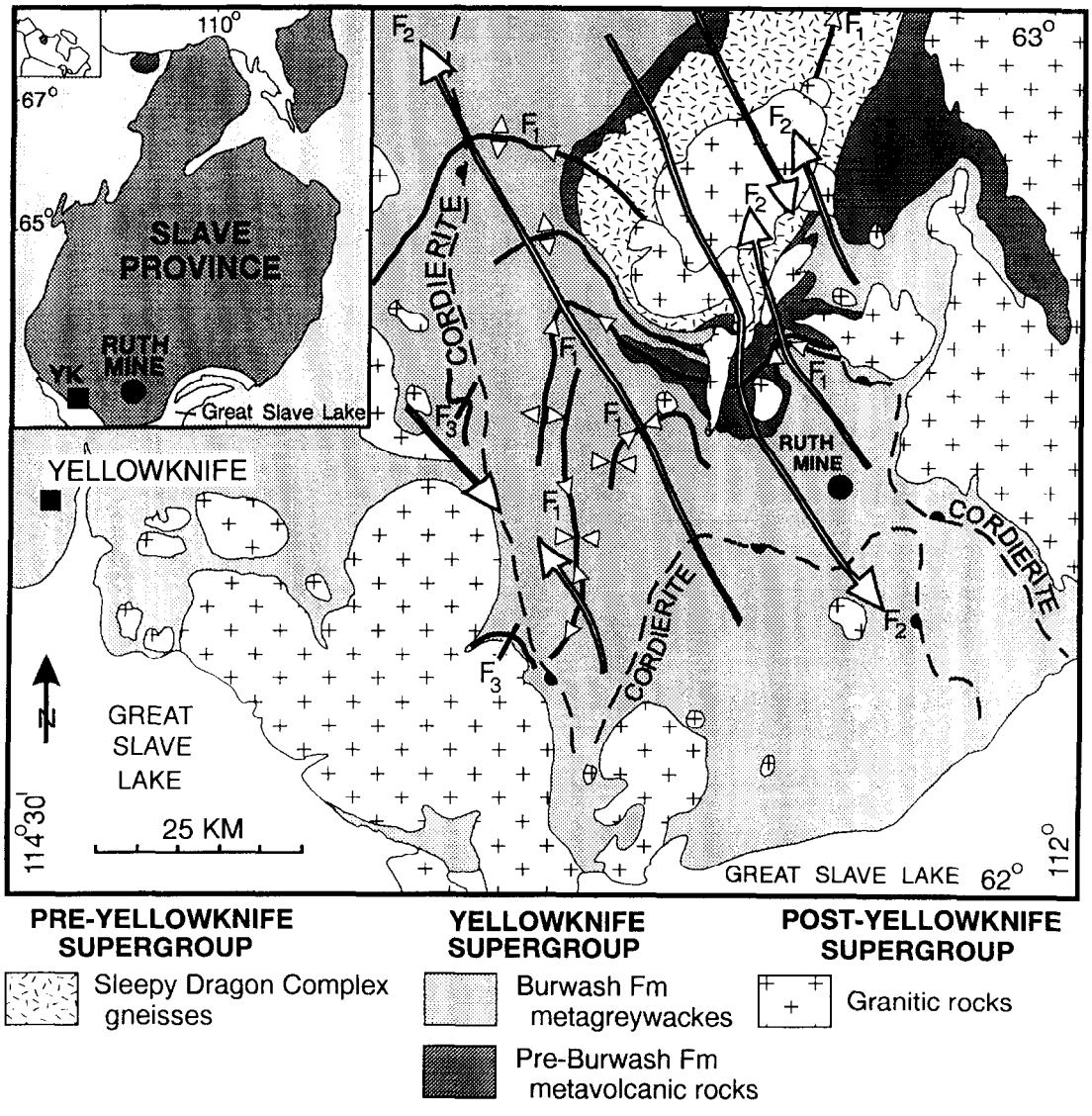

Fig. 1. Location of study area and simplified geological map of the Archean Slave structural province east of Yellowknife (YK), Canada (after Henderson, 1985 and Bleeker, 1996).

on granitoid gneisses of the Sleepy Dragon Complex. The Sleepy Dragon basement Complex has been dated at about 2.94 Ga (Lambert and van Breemen, 1991), and is significantly older than the overlying Yellowknife Supergroup volcanics and turbidites dated at about 2.66 Ga (Henderson *et al.*, 1987). Granitic batholiths and plutons intruded the supracrustal sequence between 2.62 and 2.60 Ga (Henderson *et al.*, 1987). The 2.62 Ga granites intruded the supracrustal sequence during F_2, and are coeval with the development of the regional metamorphic isograd pattern (Bleeker and Beaumont-Smith, 1995). The site of the Ruth Mine is in a regional biotite-grade metamorphic low between two cordierite-in isograds.

Three sets of macroscopic upright folds with related cleavages have been documented in the region (Bleeker and Beaumont-Smith, 1995; Bleeker, 1996). A major F_1 anticline exposes the Sleepy Dragon Complex in its breached core. Within the metaturbidites, F_1 folds are upright, tight to isoclinal periclines. F_1 folds have an S_1 slaty cleavage that is preserved in F_1 fold closures (Bleeker, 1996). The prominent folds and cleavage in the region (Fig. 1) are NNW-trending F_2 and S_2. The F_2 folds deform the regional isograds, indicating that the isograds formed before or during F_2 folding. At the Ruth Mine, absence of any preferred orientation of biotite porphyroblasts (see below) indicates that the metamorphic peak occurred under static conditions before S_2 cleavage.

Although a few macroscopic NE-trending F_3 folds in Burwash Formation metaturbidite beds have been documented by Bleeker (1996), the S_3 cleavage at the Ruth Mine is not obviously related to any macroscopic F_3 folds. According to Bleeker (pers. commun., 1996), S_3 crenulation cleavage is restricted to limbs of F_3 folds where the S_2 and S_3 display opposite vergence (chevron cleavage pattern).

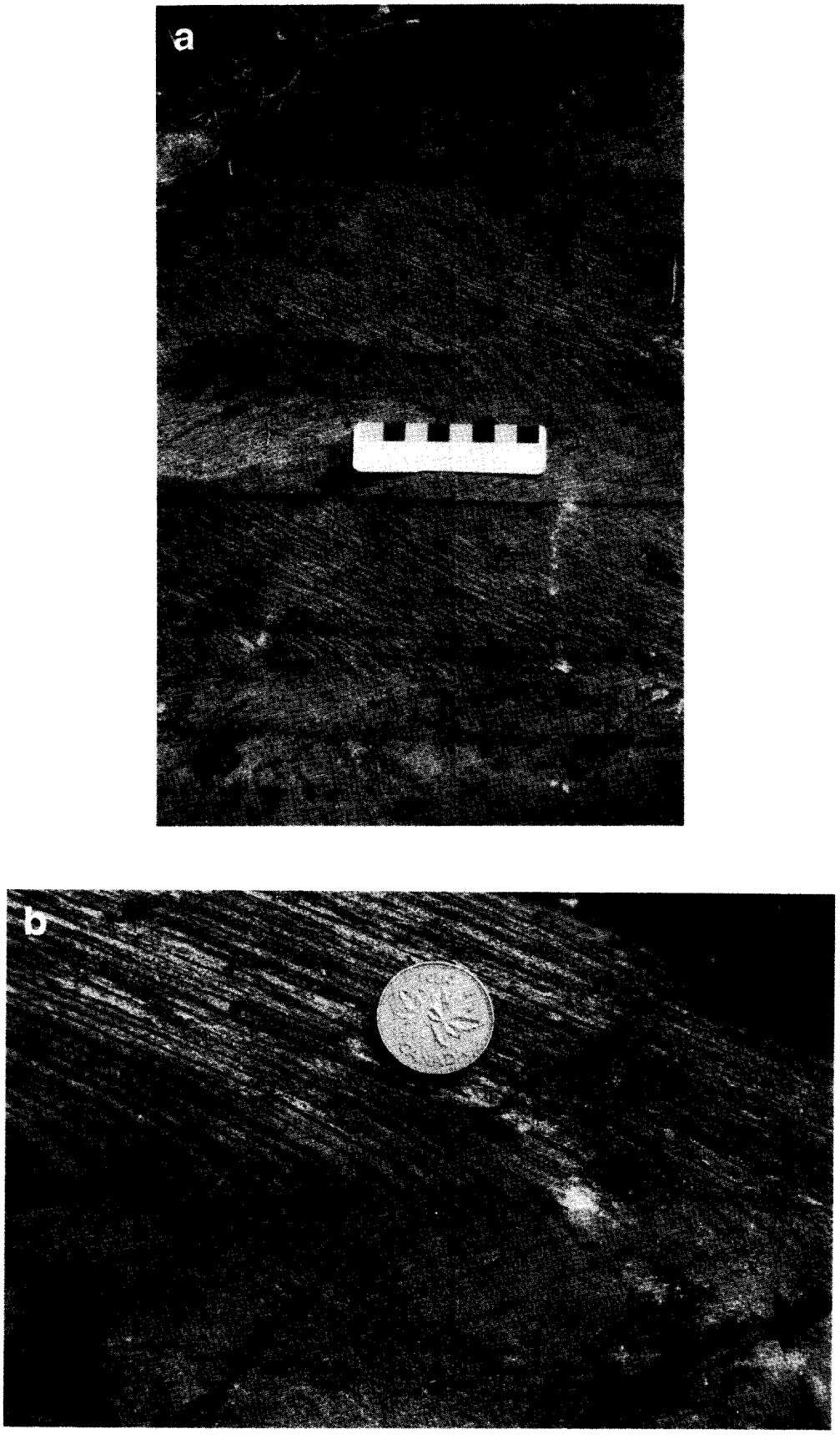

Fig. 2. Chevron cleavage pattern in vertical metaturbidite beds (N to left, parallel to bedding), continuous S_2 cleavage strikes NW in the base of the graded couplets, S_3 crenulation cleavage strikes NE in the top of the couplets. (a) Note sharp base of graded bed below scale. (b) Note progressive sinistral refraction of S_3 differentiated crenulation cleavage below coin (2 cm diameter).

CHEVRON CLEAVAGE PATTERN

The chevron cleavage pattern at the Ruth Mine comprises two generations of cleavage displaying opposite vergence in the same graded bed (Figs 2, 3 & 4a). The competent, quartz-rich bases of graded turbidite couplets retain an older continuous S_2 cleavage, and their mica-rich tops display a younger S_3 crenulation cleavage. No trace of an S_1 cleavage can be seen in the rock matrix, but is interpreted to be preserved within biotite porphyroblasts (see below).

S_3 is a compositionally differentiated cleavage exhibiting alternating quartz-rich microlithons (Q), and muscovite-rich cleavage domains (M). The width of Q domains decreases and the width of M domains increases away from the sandy bases of the graded turbidites as the S_3 cleavage refracts toward S_0. There is no evidence of an S_3 cleavage in the sandy bases of the graded beds (Fig. 4a). Using the composition of the base of the beds as a reference, it is apparent that: (1) in M domains, quartz has been selectively removed, and relict S_2 cleavage-forming muscovite and opaque material have been concentrated, and (2) in Q domains, the quartz/muscovite ratio is similar to the base of the bed, indicating that relatively little quartz has been precipitated locally in the Q domains (Fig. 4).

Together, the Q and M domains comprise S-folds that are progressively tightened toward the top of each graded bed (Figs 3 & 4a). The axial-surface traces of the asymetrical microfolds also refract (steepen) across silty laminae within metapelites (Fig. 4b). The axial-surface traces of the microfolds, and the traces of the M domains define the S_3 cleavage. In places, S_2-parallel quartz veins also define S_3 microfolds (Figs 4a top & 5a).

Many of the boundaries between Q and M domains are transitional, and relict S_2 muscovites are tiled in right-stepping, en échelon arrays in the M domains (Figs 4 & 5b–d). Some of the Q–M domain boundaries are discrete, and are defined by narrow, rough cleavage domains of mainly opaque material (Figs 4 & 5b–d). The discrete cleavage domains vary in length and width. They tend to terminate abruptly with a short right-stepping, en échelon overlap with another cleavage domain (see Fig. 4a top, and silty laminae in Fig. 4b). The kinematic significance of tiling is discussed below.

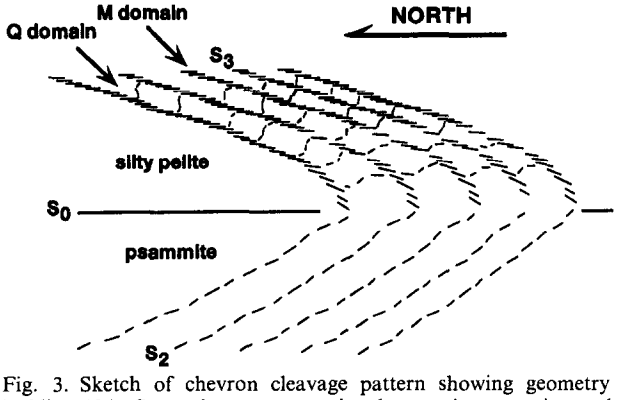

Fig. 3. Sketch of chevron cleavage pattern showing geometry of bedding (S_0), S_2 continuous muscovite cleavage in psammite, and S_3 differentiated contractional crenulation cleavage in silty pelite, forming quartz-rich microlithons (Q), and muscovite-rich cleavage domains (M). Relative to S_0, M domains form flat limbs and Q domains form steep limbs of F_3 microfolds. Note right-stepping imbrication or tiling of relict S_2 micas in M domains. Biotite porphyroblasts and continuous S_2 omitted for simplicity.

PORPHYROBLAST–MATRIX RELATIONS

Biotite porphyroblasts are less than 1.0 mm in diameter, show no preferred shape or apparent crystallographic orientation, and display S_2-parallel quartz-rich strain shadows (Figs 5b & c and 6a & b). The morphology of biotite porphyroblasts in psammite is commonly amoeboid (Fig. 6a & b), compared with porphyroblasts in metapelite which tend to have more regular margins (Fig. 6c & d). Many of the larger porphyroblasts show parallel alignment of several elliptical quartz grains, forming inclusion trails (S_i). The quartz inclusions are larger within biotite porphyroblasts in psammite than in biotite porphyroblasts in pelite (Fig. 6b & d), although the grain size of matrix quartz is uniformly greater than the quartz inclusions throughout the graded beds.

None of the S_i trails in the base of the graded beds are parallel to S_0 or S_2. The S_i is correlated with an S_1 slaty cleavage that, on a grain scale, has been destroyed in the matrix. It is preserved only within the biotite porphyroblasts, and will be referred to as S_{1i}. A few kilometers to the west of the Ruth Mine, Fyson (1980) reported similar-looking quartz S_i trails in biotite porphyroblasts which he (Fig. 4, Fyson, 1980) correlated with a continuous S_2 'first' cleavage.

The orientations of S_{1i} are related to the location of the porphyroblasts within the graded beds. For example, in Fig. 6(a), a cluster of five poikiloblastic biotites (from the base of the bed in Fig. 4a) show NE-trending S_{1i} traces compared with the NW-trending S_2 in the matrix. Figure 7(a) summarizes the orientation of S_{1i} in 32 biotite porphyroblasts from the base of the bed shown in Fig. 4(a).

Within M domains of the S_3 cleavage in the top of the bed, S_{1i} inclusion trails are NE-trending (Figs 6c & d and 7b), and are on average only slightly more northerly-trending than they are in the base of the bed (modes in Fig. 7a & b). In contrast, within Q domains (Fig. 6c & d), the S_{1i} trails trend NW with a modal cluster (Fig. 7c) that is nearly 90° discordant to the S_{1i} modes in the M domains and in the base of the bed.

DISCUSSION

The essential characteristic of the chevron cleavage pattern described here is the preservation of an older fabric in more competent bases of graded couplets with a vergence opposite to a younger crenulation cleavage

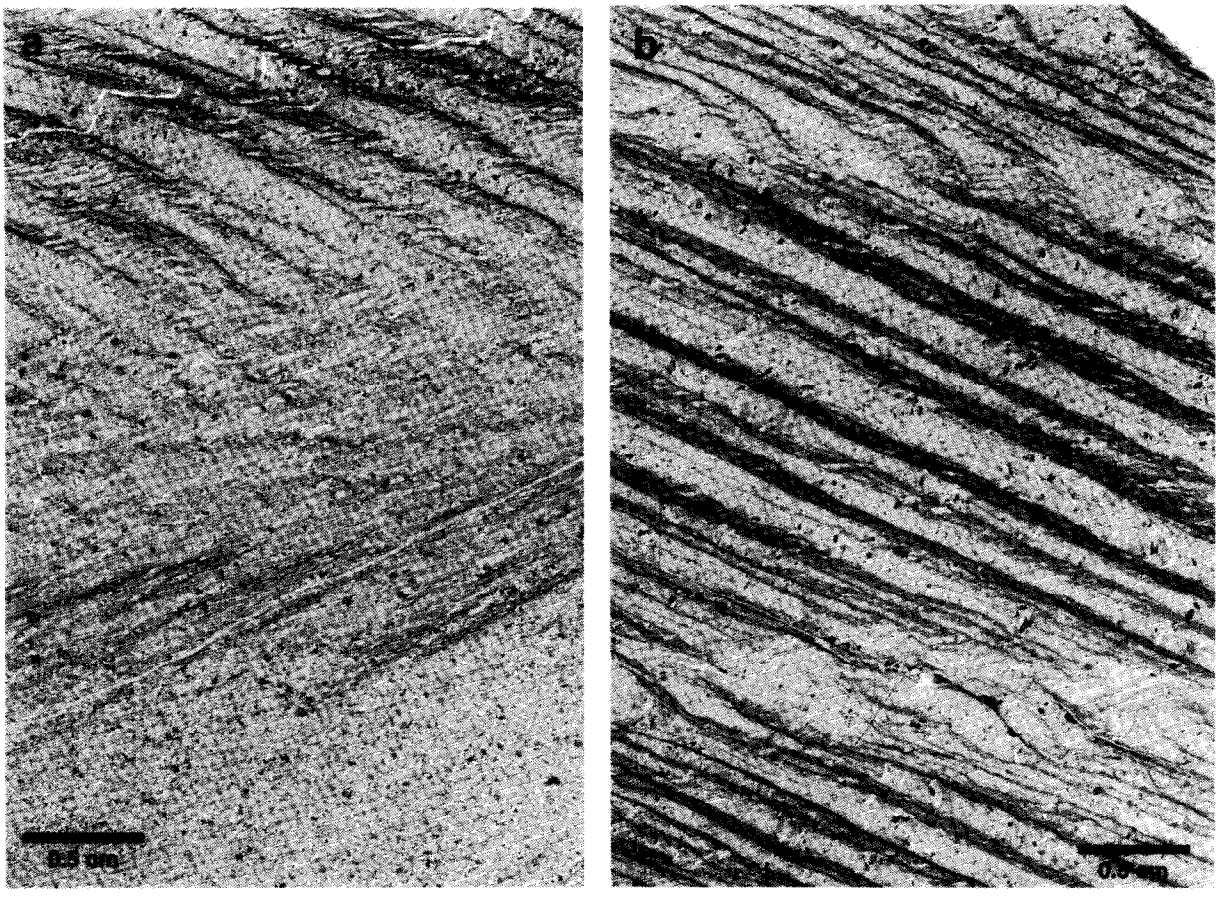

Fig. 4. Photomicrographs (ppl) of metaturbidite (N to left, parallel to scale bar). S_0 strikes 360° parallel to scale bar. Beds young to the east. (a) S_2–S_3 chevron cleavage pattern. Continuous S_2 cleavage in psammite (S_2 trace about 335°) in lower half of photomicrograph. Differentiated S_3 crenulation cleavage in semi-pelite (S_3 trace about 025°) in upper half of photomicrograph. Dark spots are biotite porphyroblasts. Folded S_2-parallel quartz vein at top of photomicrograph is drawn in Fig. 7. Pale, S_2-parallel bands are quartz-rich strain shadows adjacent to competent pre-S_2 biotite porphyroblasts. (b) S_3 crenulation cleavage in semi-pelitic top of graded couplet. Note S_3 refracts (i.e. steepens relative to S_0) across two 0.5 cm-wide silty laminae near top and bottom of photomicrograph shown by progressive opening of F_3 microfold interlimb angles and steepening of axial-surface traces.

developed in less-competent tops of graded beds. The chevron cleavage pattern records a component of sinistral bedding-parallel shear during D_3 that caused the S_2 cleavage to shorten by buckle-folding. The sinistral shear was partitioned into the less-competent silty-pelite comprising the tops of graded beds, and formed asymmetrical S-microfolds in S_2.

The folded S_2-parallel quartz vein shown at the top of Fig. 4(a) records a bedding-parallel sinistral shear strain of 0.18, and about 10% shortening normal to S_3 (Fig. 8). The enveloping surface of the folded S_2-parallel quartz vein (Figs 4a & 8) is slightly less-steeply inclined counter-clockwise to S_0 than the undeformed S_2 in the base of the bed. This indicates that S_2 enveloping surfaces in the top of the bed have not been rotated significantly during D_3 sinistral shear, and S_3 is not transposed S_2.

The asymmetrical F_3 microfolds indicate significant partitioning of strain between rotation and pressure solution within the semi-pelitic top of the beds. The Q domains show a progressive rotational strain regime within the microlithons. As the S_3 cleavage refracts toward S_0, the S_2 micas in the Q domains are progressively rotated counter-clockwise as the S-microfolds tighten. On the other hand, the M domains indicate significant dissolution–removal of quartz. Here, relict S_2 micas have collapsed upon each other forming a characteristic right-stepping imbricated layering or tiling (Figs 3, 4 & 5). Tiling of micas is a common feature in M domains of differentiated crenulation cleavages (plates 25, 26, 40, and 44 in Borradaile *et al.*, 1982; figs 4.11, 4.12 and 11.3 in Passchier and Trouw, 1995), and provides a reliable shear criterion. Tiling in M domains of contractional crenulation cleavage should not be confused with tiling in extensional crenulation cleavage (shear bands) commonly observed in mylonites. Extensional crenulations exhibit tiling in cleavage domains, but indicate a shear sense opposite to that inferred from contractional crenulations (see Passchier and Trouw, 1995, p. 112). The rocks described here show very low strains compared with mylonites,

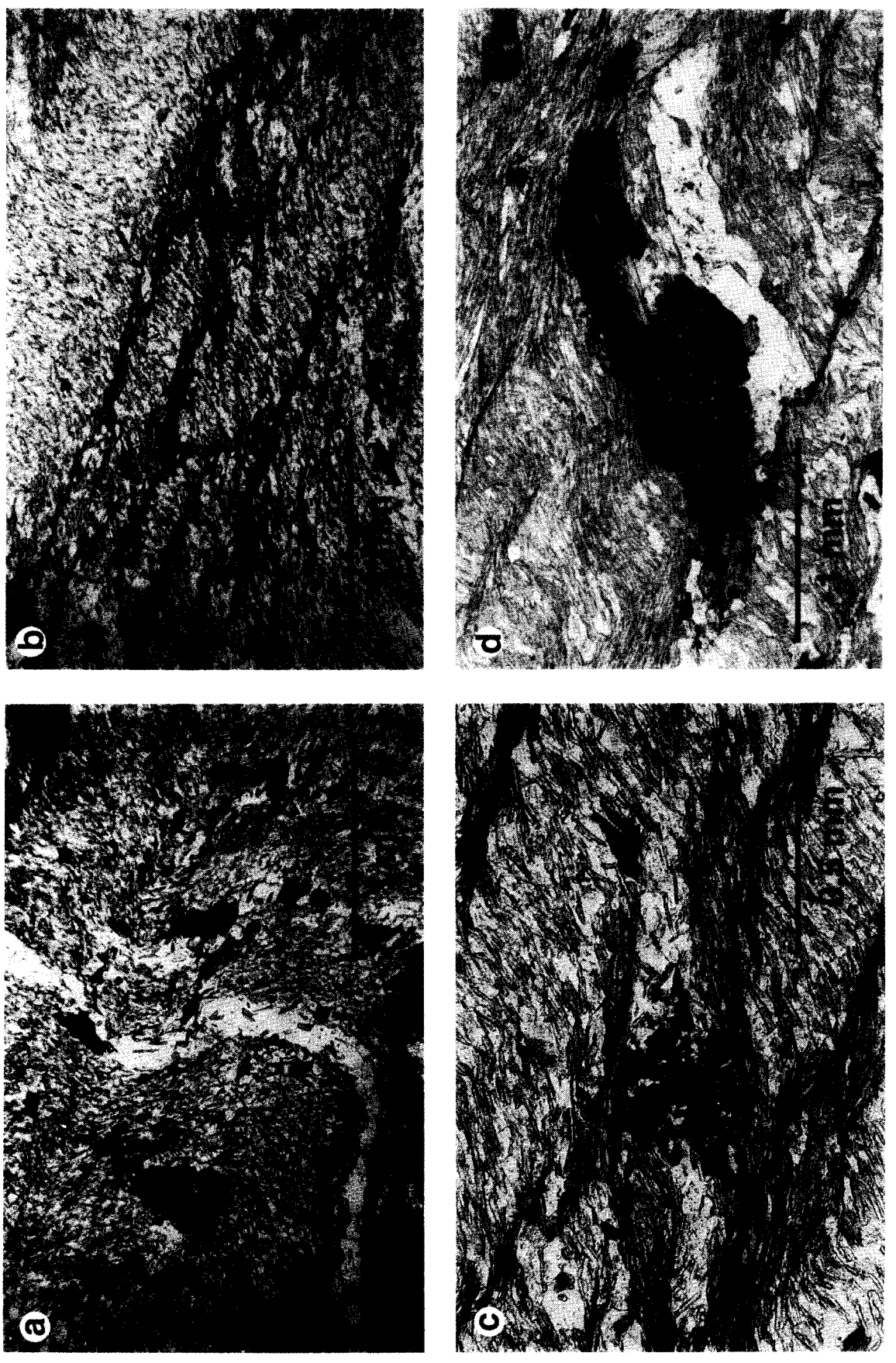

Fig. 5. Photomicrographs (ppl) of S_3 crenulation cleavage (N to left). (a) Folded S_2-parallel quartz vein (enlargement of vein shown near top-left of Fig. 4a) with steep segment in microlithon (Q domain) and flat segment in M domain. (b) F_3 microfolds defined by deformed S_2 muscovites, and folded quartz-rich strain shadows adjacent to biotite porphyroblast (near right-centre of photomicrograph). Note right-stepping tiling of short M domain segments. (c) Enlarged view of biotite porphyroblast in Fig. 5b showing folded delta-like quartz-rich strain shadow adjacent to porphyroblast, and transition from M to Q domains forming open S-microfolds. (d) Competent mass of opaque material, biotite porphyroblast and strain-shadow quartz showing buttressing and refraction of S_3 crenulation cleavage. Note S_3 domains are both transitional and discrete.

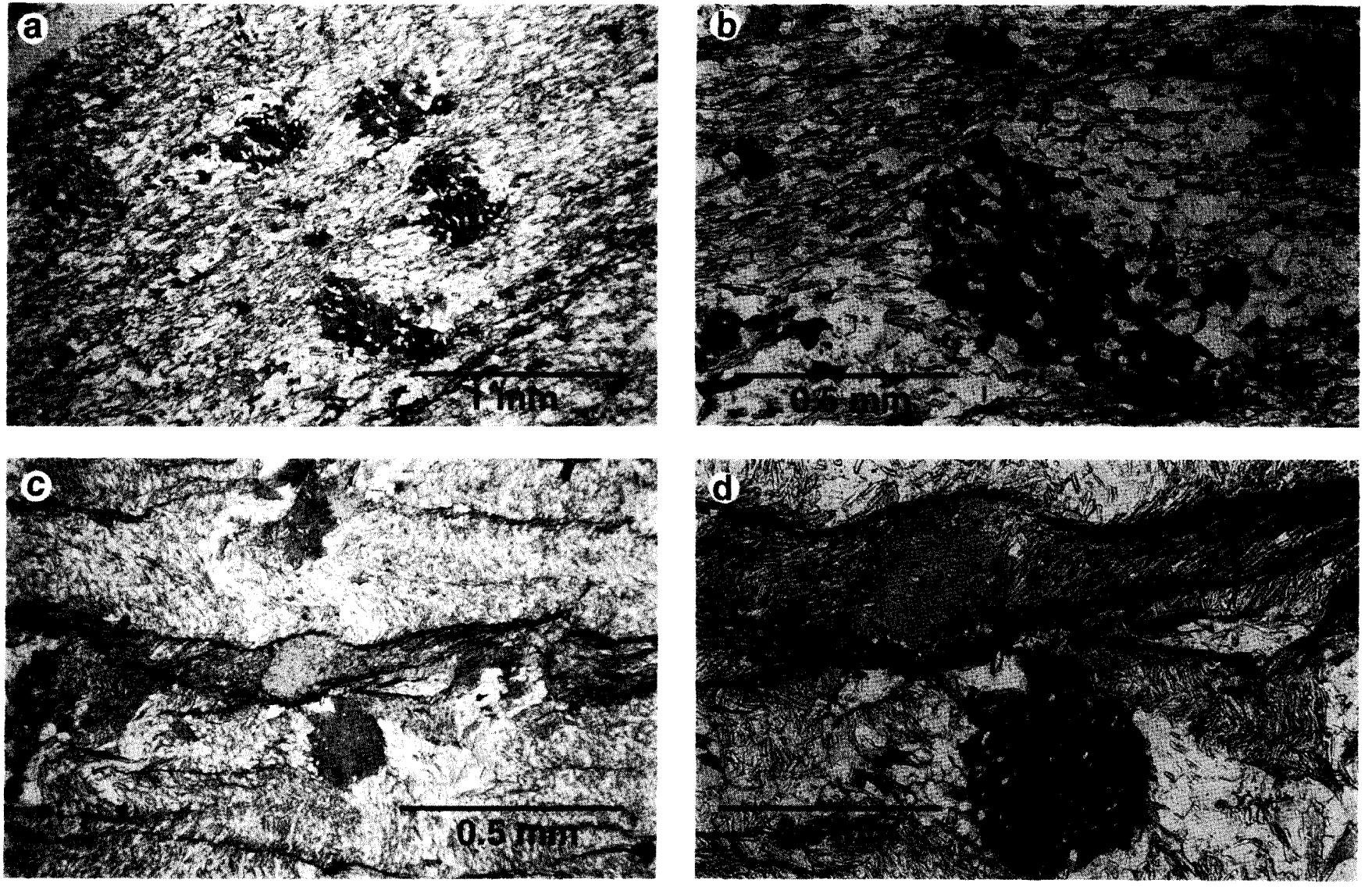

Fig. 6. Photomicrographs (ppl) of porphyroblast–matrix relations (N to left). (a) Metapsammite showing a cluster of five poikiloblastic biotites with NE-trending S_{li} traces defined by aligned elliptical quartz inclusions, wrapped by NW-trending continuous S_{2e} matrix fabric of muscovite and elliptical quartz grains. (b) Enlarged view of lower biotite porphyroblast in cluster shown in Fig 6a. (c) S_3 crenulation cleavage with biotite porphyroblasts in M and Q domains (centre of photomicrograph). (d) Enlarged view of biotite porphyroblasts shown in (c). Note S_i in porphyroblast within the M domain trend NE, and S_i in the porphyroblast within the Q domain trend NW.

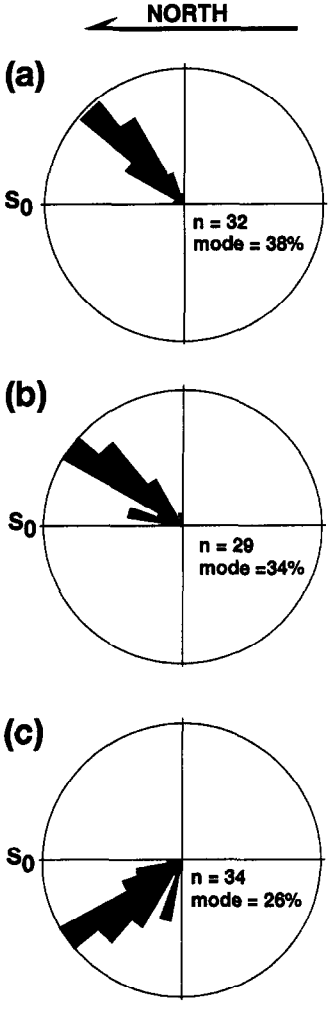

Fig. 7. Rose diagrams showing geometry of S_{li} in 95 biotite porphyroblasts from 3 oriented thin sections of graded metaturbidite shown in Fig. 2b. Sections are horizontal, perpendicular to intersection of S_0, S_2 and S_3. (a) S_{li} traces from 32 biotite porphyroblasts in psammitic part of bed. (b) S_{li} traces from 29 biotite porphyroblasts in M-domains of pelitic part of bed. (c) S_{li} traces from 34 biotite porphyroblasts in Q-domains of pelitic part of bed.

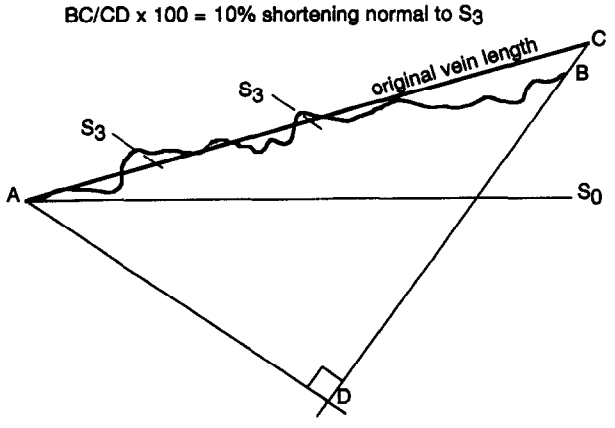

Fig. 8. Estimation of 10% shortening perpendicular to S_3-cleavage by comparing the original (AB) and folded (AC) length of the S_2-parallel quartz vein shown in Fig. 4(a). The bedding-parallel shear strain indicated by the folded vein is 0.18.

although folding of S_2-parallel quartz-rich strain shadows (Fig. 5b & c) is analogous kinematically to rotation of delta-type porphyroclasts in mylonites (Passchier and Simpson, 1986).

These interpretations of S_3 development are supported by the data on porphyroblast–matrix S_i–S_e relations. Assuming that the geometry of quartz-inclusion trails in biotites from the base of the bed shown in Fig. 4(a) are unaffected by the D_3 strain recorded by the S_3 cleavage in the top of the bed, the similar orientation of S_{1i} in biotites in M domains compared with their orientation in the base of the bed (Fig. 7a & b) suggests that within the M domains, strain was largely irrotational with respect to the enclosed biotite porphyroblasts. Within Q domains, the strong discordance of the S_{1i} in biotites relative to those in the base of the bed argues for porphyroblast rotation coupled to rotation of relict S_2 micas in the S_3 microlithons.

Compared with the orientation of S_2 in the base of the bed, the average rotation of the steep limbs of the microfolds (Q domains) is about 90° counter-clockwise, and the rotation of the flat limbs of the microfolds (M domains) is about 5° clockwise. It should be noted that this discussion does not consider refraction of S_2 prior to S_3 development. However, S_2 refraction would not affect the conclusion that S_2 and the biotite porphyroblasts have rotated, on average, at least 90° counter-clockwise on the steep limbs of F_3 microfolds. On the other hand, the 5° clockwise discordance of the S_2 micas in the M domains may be a relict of S_2 refraction preserved in the flat limbs of the F_3 microfolds relative to the steep limbs, or it may be explained by 'back rotation' due to volume loss during solution-removal of quartz from the flat limbs of the F_3 microfolds.

CONCLUSIONS

Chevron cleavage pattern is characterized by two cleavages of opposite vergence mirrored by a bedding plane. The bedding plane may be a zone of mechanical continuity where the bed is a graded turbidite. In this study, an S_2 cleavage is preserved in the more competent psammitic bases of graded turbidites, and an S_3 differentiated crenulation cleavage is developed in the less competent semi-pelitic tops of the beds. Progressively increasing strain toward the top of a graded bed is indicated by progressive refraction of the S_3 crenulation cleavage.

The S_3 crenulations formed by microfolding of S_2 cleavage. Bedding-parallel shear caused shortening and folding of the cleavage where the older cleavage was in the F_3/D_3 shortening field, thus forming the chevron cleavage pattern. Where the S_2 and S_3 cleavages verge in the same sense relative to bedding, the S_2 cleavage is reinforced and no S_3 crenulation cleavage develops. In this example, the F_3 microfolds are asymmetrical S-folds of S_2. The steep limbs define quartz-rich Q domains, and

the flat limbs define muscovite-rich M domains. The Q domains are deformed microlithons within which little apparent compositional change has occurred, but the S_{1i} and S_2 fabrics have been rotated about 90° counter-clockwise from their apparent original orientations in the base of the bed. The M domains are zones of quartz dissolution and concentration of relict S_2 muscovite and insoluble opaque material. The relict S_2 muscovites form a characteristic right-stepping offset layering or tiling that has kinematic significance in differentiated metamorphic layering formed by microfolding. S-folds are due to sinistral shear and Z-folds are due to dextral shear of the S_2 cleavage. Both asymmetrical microfolds and tiling of relict micas reveal the D_3 shear sense within the tops of the graded couplets.

Biotite porphyroblasts occur throughout the graded beds. The porphyroblasts grew statically before the development of the S_2 cleavage, and contain quartz-inclusion trails that are discordant to the matrix S_2 cleavage, as well as S_0. The trails are interpreted to preserve an S_1 slaty cleavage in the rock (i.e. S_{1i}). The S_{1i} have a strong preferred orientation in each part of the graded bed: NE in the base, NE in the M domains of the differentiated crenulation cleavage, and NW in the Q domains. It is apparent from these observations that biotite porphyroblasts within the Q domains rotated about 90° counter-clockwise during S-microfolding. Within the M domains, the S_{1i} data suggest that the porphyroblasts may have rotated clockwise about 5°, relative to their orientation in the base of the beds, possibly due to solution-removal of quartz from M domains of S_3. Alternatively, they may preserve an original S_2 refraction in the more pelitic part of the beds. In any case, within M domains, biotite porphyroblasts have not rotated significantly.

In this example, a clear transition can be seen between M and Q domains comprising the flat and steep limbs of asymmetrical F_3 microfolds. Also in this example, a bimodal distribution of S_{1i} in biotite porphyroblasts contained within Q domains is characteristic of porphyroblast rotation coupled to F_3 microfolding of S_2 foliation.

Acknowledgements—I am indebted to John Brophy who recognized the chevron cleavage pattern whilst mapping around the Ruth Mine, and brought it to my attention. Reviews by Steve Lucas, Wouter Bleeker, Bill Fyson, Tom Wright, Frank Fueten, Shoufa Lin, and Mariette Henderson significantly improved the clarity and organization of the manuscript. I thank Associate Editor Joe White, and referees Steve Ralser and Eric Erslev for constructive comments. This is Geological Survey of Canada Contribution 1996384.

REFERENCES

Aerden, D. G. A. M. (1995) Porphyroblast non-rotation during crustal extension in the Variscan Lys-Callaouas massif, Pyrenees. *Journal of Structural Geology* **17**, 709–725.

Bell, T. H. (1985) Deformation partitioning and porphyroblast rotation in metamorphic rocks: a radical re-interpretation. *Journal of Metamorphic Geology* **3**, 109–118.

Bell, T. H. and Johnson, S. E. (1992) Shear sense: a new approach that resolves conflicts between criteria in metamorphic rocks. *Journal of Metamorphic Geology* **10**, 99–124.

Bleeker, W. (1996) Thematic structural studies in the Slave Province, Northwest Territories: the Sleepy Dragon Complex. In *Current Research 1996-C*, 37–48. Geological Survey of Canada.

Bleeker, W. and Beaumont-Smith, C. (1995) Thematic structural studies in the Slave Province: preliminary results and implications for the Yellowknife Domain, Northwest Territories. In *Current Research 1995-C*, 87–96. Geological Survey of Canada.

Borradaile, G. J., Bayly, M. B. and Powell, C. M. (editors) (1982) *Atlas of Deformational and Metamorphic Rock Fabrics*. Springer-Verlag, New York.

Fyson, W. K. (1980) Fold fabrics and emplacement of an Archean granitoid pluton, Cleft Lake, Northwest Territories. *Canadian Journal of Earth Sciences* **17**, 325–332.

Fyson, W. K. (1982) Complex evolution of folds and cleavages in Archean rocks, Yellowknife, NWT. *Canadian Journal of Earth Sciences* **19**, 878–893.

Henderson, J. B. (1985) Geology of the Yellowknife–Hearne Lake area, District of Mackenzie, Northwest Territories: a segment across an Archean basin. *Geological Survey of Canada Memoir* 414, Geological Survey of Canada.

Henderson, J. B., van Breemen, O. and Loveridge, W. D. (1987) Some U–Pb zircon ages from Archean basement, supracrustal and intrusive rocks, Yellowknife–Hearne Lake area, District of Mackenzie. In *Radiogenic Age and Isotope Studies: Report 1*, Geological Survey of Canada Paper 87-2, 111–121.

King, J. E. and Helmstaedt, H. (1989) Deformational history of an Archean fold belt, eastern Point Lake, Slave structural province, N.W.T. *Canadian Journal of Earth Sciences* **26**, 106–118.

Kusky, T. M. and De Paor, D. G. (1991) Deformed sedimentary fabrics in metamorphic rocks: Evidence from the Point Lake area, Slave province, Northwest Territories. *Geological Society of America Bulletin* **103**, 486–503.

Lambert, M. L. and van Breemen, O. (1991) U–Pb zircon ages from the Sleepy Dragon Complex and a new occurrence of basement rocks within the Meander Lake Plutonic Suite, Slave Province, N.W.T. In *Radiogenic Age and Isotope Studies: Report 4*, Geological Survey of Canada Paper 90-2, 78–94.

Passchier, C. W. and Simpson, C. (1986) Porphyroclast systems as kinematic indicators. *Journal of Structural Geology* **8**, 831–843.

Passchier, C. W. and Trouw, R. A. J. (1995) *Microtectonics*. Springer, New York.

Vissers, P. and Mancktelow, N. S. (1992) The rotation of garnet porphyroblasts around a single fold, Lukmanier Pass, Central Alps. *Journal of Structural Geology* **14**, 1193–1202.